Contract No:

This document was prepared in conjunction with work accomplished under Contract No. DE-AC09-08SR22470 with the U.S. Department of Energy.

Disclaimer:

Ceramic Waste Form Data Package

Fuel Cycle Research & Development

Prepared for
U.S. Department of Energy Office of Nuclear Energy
Separations and Waste Forms Campaign

J.W. Amoroso and J.C. Marra
Savannah River National Laboratory

June 13, 2014

FCRD-SWF-2014-000581
SRNL-STI-2014-00247

APPROVALS

AUTHORS:

J.W. Amoroso — Date
SRNL Process Technology Programs

C.C. Marra — Date
SRNL Materials Science and Technology

REVIEWERS:

D. K. Peeler, Technical Reviewer — Date
SRNL Process Technology Programs

D. H. McGuire, Management Reviewer — Date
Manager, SRNL Process Technology Programs

SUMMARY

The purpose of this data package is to provide information about simulated crystalline waste forms that can be used to select an appropriate composition for a Cold Crucible Induction Melter (CCIM) proof of principle demonstration. Melt processing, viscosity, electrical conductivity, and thermal analysis information was collected to assess the ability of two potential candidate ceramic compositions to be processed in the Idaho National Laboratory (INL) CCIM and to guide processing parameters for the CCIM operation. Given uncertainties in the CCIM capabilities to reach certain temperatures throughout the system, one waste form designated 'Fe-MP' was designed towards enabling processing and another, designated 'CAF-5%TM-MP' was designed towards optimized microstructure.

Melt processing studies confirmed both compositions could be poured from a crucible at 1600°C although the CAF-5%TM-MP composition froze before pouring was complete due to rapid crystallization (upon cooling). X-ray diffraction measurements confirmed the crystalline nature and phase assemblages of the compositions. The kinetics of melting and crystallization appeared to vary significantly between the compositions. Impedance spectroscopy results indicated the electrical conductivity is acceptable with respect to processing in the CCIM.

The success of processing either ceramic composition will depend on the thermal profiles throughout the CCIM. In particular, the working temperature of the pour spout relative to the bulk melter which can approach 1700°C. The Fe-MP composition is recommended to demonstrate proof of principle for crystalline simulated waste forms considering the current configuration of INL's CCIM. If proposed modifications to the CCIM can maintain a nominal temperature of 1600°C throughout the melter, drain, and pour spout, then the CAF-5%TM-MP composition should be considered for a proof of principle demonstration.

CONTENTS

FIGURES

TABLES

ABBREVIATIONS

A	slope of Arrhenius equation
B	intercept of Arrhenius equation
CCIM	cold crucible induction melter
DTA	differential thermal analysis
η	viscosity
g	gram(s)
INL	Idaho National Laboratory
M	molar
σ	electrical conductivity
SRNL	Savannah River National Laboratory
T	temperature
Wt. %	weight percent
XRD	X-ray diffraction

ACKNOWLEDGEMENTS

The authors thank Phyllis Workman and David Missimer from SRNL for assistance with sample preparation and property measurements and Jarrod Crum from PNNL for providing electrical conductivity measurement data.

This work was supported by the U.S. Department of Energy, Office of Nuclear Energy, under Contract DE-AC02-06CH11357.

1. INTRODUCTION

A multi-phase ceramic waste form is being developed at the Savannah River National Laboratory (SRNL) for treatment of secondary waste streams generated by reprocessing commercial spent nuclear. The envisioned waste stream contains a mixture of transition, alkali, alkaline earth, and lanthanide metals. Ceramic waste forms are tailored (engineered) to incorporate waste components as part of their crystal structure based on knowledge from naturally found minerals containing radioactive and non-radioactive species similar to the radionuclides of concern in wastes from fuel reprocessing. The ability to tailor ceramics to mimic naturally occurring crystals substantiates the long term stability of such crystals (ceramics) over geologic timescales of interest for nuclear waste immobilization [1]. A durable multi-phase ceramic waste form tailored to incorporate all the waste components has the potential to broaden the available disposal options and thus minimize the storage and disposal costs associated with aqueous reprocessing.

Multi-phase ceramics are designed to crystallize upon cooling from a melt. Compositions are designed based on combinations of the waste and additives to target desired hollandite, perovskite, and pyrochlore phases upon melting. Elements with a +3 or +2 valance form perovskite ((A+2)TiO3) and pyrochlore ((A+3)2Ti2O7) type phases [2, 3]. Zirconium (+4 valence) partitions to a zirconolite (CaZrTi2O7) phase [4]. Cs and Rb elements partition to a hollandite structure based on the general formula BaxCsyMzTi+48-zO16 where z = 2x+y for trivalent cations and z = x+y/2 for divalent cations for charge compensation [5-7].

Idaho National Laboratory (INL) plans to conduct a cold crucible induction melter (CCIM) test in FY2014 with ceramic waste form(s) developed at SRNL to demonstrate proof of principle for processing multi-phase crystalline simulated waste form. Multi-phase ceramic compositions targeting Fe-, Cr-, and Cr/Al/Fe- based hollandite have been developed at SRNL on a laboratory scale for ultimate processing using CCIM technology. In general, the Cr-, and Cr/Al/Fe- based compositions have been shown to form desirable phase assemblages whereas the Fe-based compositions have significant parasitic non-durable phases [8]. However, higher temperatures are needed to melt process the Cr- and Cr/Al/Fe- based compositions compared to the Fe-based compositions. Currently, the INL CCIM is configured to process lower melting glasses and glass-ceramics. Crystalline ceramics require higher nominal melting temperatures and increase the risk of freezing (crystallization) during processing especially in the pour spout which is temperature gradients are limited by the CCIM design. Considering the nature of melt processing ceramics and uncertainties in the INL's CCIM capabilities (e.g. pour spout temperature) two ceramic compositions were developed and tested to support a proof of principle CCIM test.

This document is a data package summarizing laboratory experiments and results designed to support the proof of principle CCIM test. The data provided in this document is intended assist selecting a composition(s) suitable for processing in the CCIM available at INL. Melt processing, viscosity, electrical conductivity, and thermal analysis information was collected to assess the ability of each waste form to be processed in INL's CCIM and to guide required processing parameters for the CCIM operation.

2. EXPERIMENTAL

Unlike the glasses and glass-ceramics that have been processed in INL's CCIM, the ceramic compositions discussed in this report melt at higher temperatures and require a minimum temperature be maintained throughout processing to prevent permanent crystallization (solidification). Successful processing and proof of principle includes, melt initiation, melting, controlled pouring (stopping and starting), and post draining. Discussions with INL personnel indicated that the CCIM's current pour spout design will limit the processing capability for ceramics such as those developed at SRNL.

Two ceramic compositions were developed and tested considering INL's CCIM capabilities. One, designated 'Fe-MP' was designed towards optimized processing and the other, designated 'CAF 5%TM MP' was designed towards optimized microstructure. The Fe-MP composition which, was an early developed composition and is known to melt at lower temperatures but suffers from improper phase assemblage, is expected to be adequate for processing in the CCIM as currently configured at INL. The CAF-5%TM-MP composition was formulated based on a baseline Cr/Al/Fe-based hollandite composition but with 5% addition of transition metal (TM) elements in an effort to enhance melt-ability for processing in the CCIM. The CAF-5%TM-MP composition forms proper phases upon cooling but still melts at higher temperatures and may test the limits of INL's CCIM.

The two compositions studied are listed on an oxide basis in Table 1.

Table 1. Target Oxide Concentrations (wt. %) in Ceramic Waste Form.

Component	Fe-MP	CAF-5%TM-MP
Al_2O_3	0.00	1.25
CaO	1.37	1.75
CdO	0.11	0.11
Cr_2O_3	0.00	6.23
Eu_2O_3	0.17	0.17
Fe_2O_3	15.13	6.55
Gd_2O	0.16	0.16
SrO	0.97	0.96
TiO_2	48.65	49.48
ZrO_2	2.96	3.06
BaO	12.63	12.57
Ce_2O_3	3.07	3.03
Cs_2O	2.85	2.81
La_2O_3	1.57	1.55
MoO_3	0.84	0.83
Nd_2O_3	5.18	5.11
Pr_2O_3	1.43	1.41
SeO_2	0.08	0.08
SnO_2	0.07	0.07
Sm_2O_3	1.07	1.05
TeO_2	0.65	0.67
Y_2O_3	0.62	0.64
Rb_2O	0.42	0.43

2.1. Melt Processing

The melt and pour behavior of the compositions was studied using 15g and 300g batches. Raw material (carbonates and oxides) was loosely placed into a covered alumina crucible. The 300g batches were intended as a laboratory scale-up (compared to the 15g batches) and provided material for subsequent electrical characterization. The samples were heated in air at approximately 10°C/min, held at 1600°C for 20 minutes, removed from the furnace, and immediately poured into a stainless steel mold.

2.2. Viscosity

Viscosity as a function of temperature was measured for both compositions. The SRNL procedure [9] used to measure viscosity is in accordance with the American International C965 Procedure A in which the viscosity is measured using a rotating spindle and a fixed crucible. A portion of pre-melted (see Section 2.1) material was placed in a Pt/Rh-crucible and heated in a high temperature furnace. A Pt/Rh bob was lowered into the melt at a fixed temperature and rotated. After steady-state conditions were obtained, the torque required to rotate the bob at a constant speed was recorded with a Brookfield viscometer. A series of such torque measurements at various temperatures was then converted to viscosities to obtain viscosity as a function of temperature for each composition. Torque conversions were made using experimentally derived instrument constants developed specifically to the SRNL system and verified with reference standards [10, 11].

The temperature was initially set to achieve a melt (or a liquid-solid solution) in which the spindle bob could be lowered. The temperature was then decreased incrementally until viscosity increased beyond the instrument capability. Subsequently, a duplicate measurement was taken near the melting temperature to confirm the reversibility of the viscosity behavior. Instrument detection limits and crystallization in the melt limited the range of temperatures over which quality viscosity measurements could be obtained.

2.3. Electrical Conductivity

Impedance spectroscopy was performed on the FE-MP composition over a temperature range of 1550°C to 1300°C according to an established procedure [12]. Data was collected incrementally at several temperatures. Triplicate impedance measurements were performed at each temperature after a 20 – 30 minute isothermal dwell. The impedance analyzer was calibrated "as a system" with 0.1 M and 1 M KCl reference solutions at room temperature to determine the cell constant per the procedure. Impedance spectroscopy was not performed on the CAF-5%TM-MP sample due to inadequate melting observed at 1585°C (maximum working range of the impedance setup).

2.4. Thermal Analysis

Differential Thermal Analysis (DTA) was performed on both compositions using a Netzsch STA 409 PC Luxx system [14]. Specimens taken from material that was melted and poured (see section 3.1) were heated at 20 K/min. to 1500°C, held at 1500°C for 5 min., and cooled at 20 K/min. to 200°C. Samples were heated in covered alumina crucibles with flowing air.

3. RESULTS & DISCUSSION

3.1. Melt Processing

Both the Fe-MP and CAF-5%TM-MP compositions poured from the crucible at 1600°C. The Fe-MP melt was visually very fluid (self-leveling) and all the material poured from the crucible excepting a thin film which lined the crucible inside. The CAF-5%TM-MP melt was comparatively less fluid as evidenced by a significant portion of material remaining in the crucible and non-uniform mold filling. Presumably that

composition crystallized sufficiently rapidly as the melt cooled during pouring such that not all the material flowed out of the crucible. Additionally, visual inspection of the CAF-5%TM-MP suggested that a high temperature needle-like crystalline phase persisted in equilibrium with the liquid at 1600°C as evidenced by a network of needle-like crystals remaining in the crucible as though a liquid was decanted from the crucible leaving the needle-like crystals. A less pronounced but similar microstructure was observed in the Fe-MP composition that suggests a similar phenomenon occurs in the Fe-MP composition but, is suppressed by kinetic effects (see Section 4**Error! Reference source not found.**). X-ray diffraction (XRD) revealed that the needle-like crystals were rich in hollandite but, perovskite and pyrochlore phases were also present. It is unknown if the perovskite and pyrochlore were caused from contamination during sampling or if the crystal matrix contained all phases. Digital images of the two patties from the 300g pours are shown in Figure 1. Both materials were crystalline consisting of multiple phases as evidenced by the XRD patterns in Figure 2. The CAF-5%TM-MP composition exhibited the expected hollandite, perovskite, and pyrochlore phases upon cooling whereas the Fe-MP sample exhibited major and minor phases in addition to expected hollandite, perovskite, and pyrochlore phases [8, 15, 16].

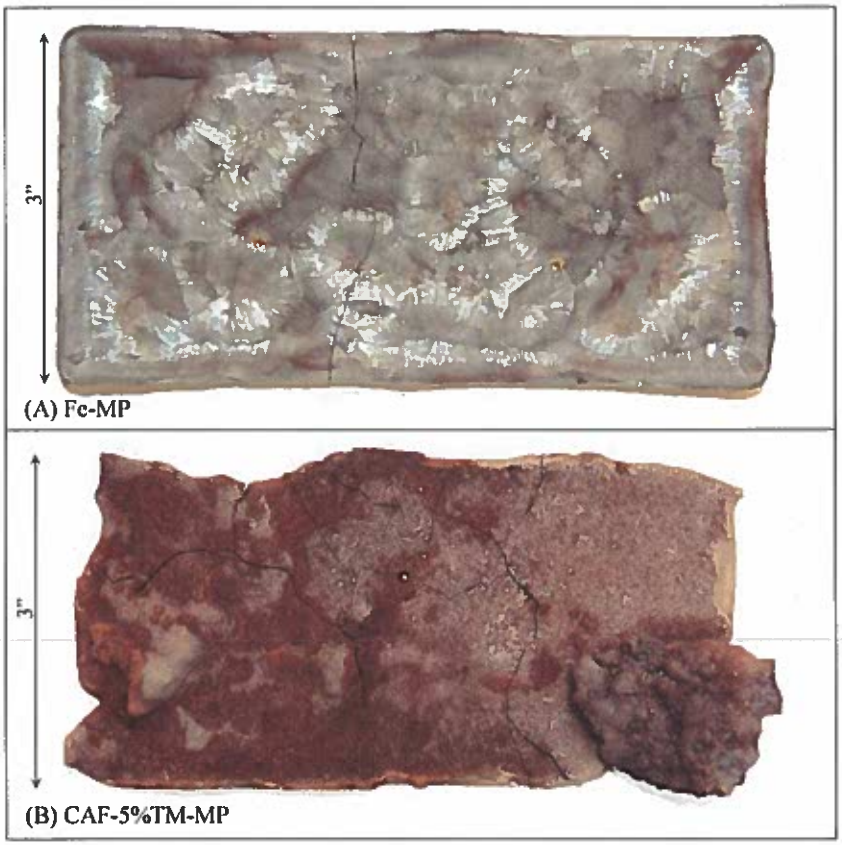

Figure 1. Image of (A) Fe-MP pour patty and (B) CAF-5%TM-MP pour patty. (The clump of material in the bottom right corner of (B) is crystallized material that was the last material to pour out the crucible.

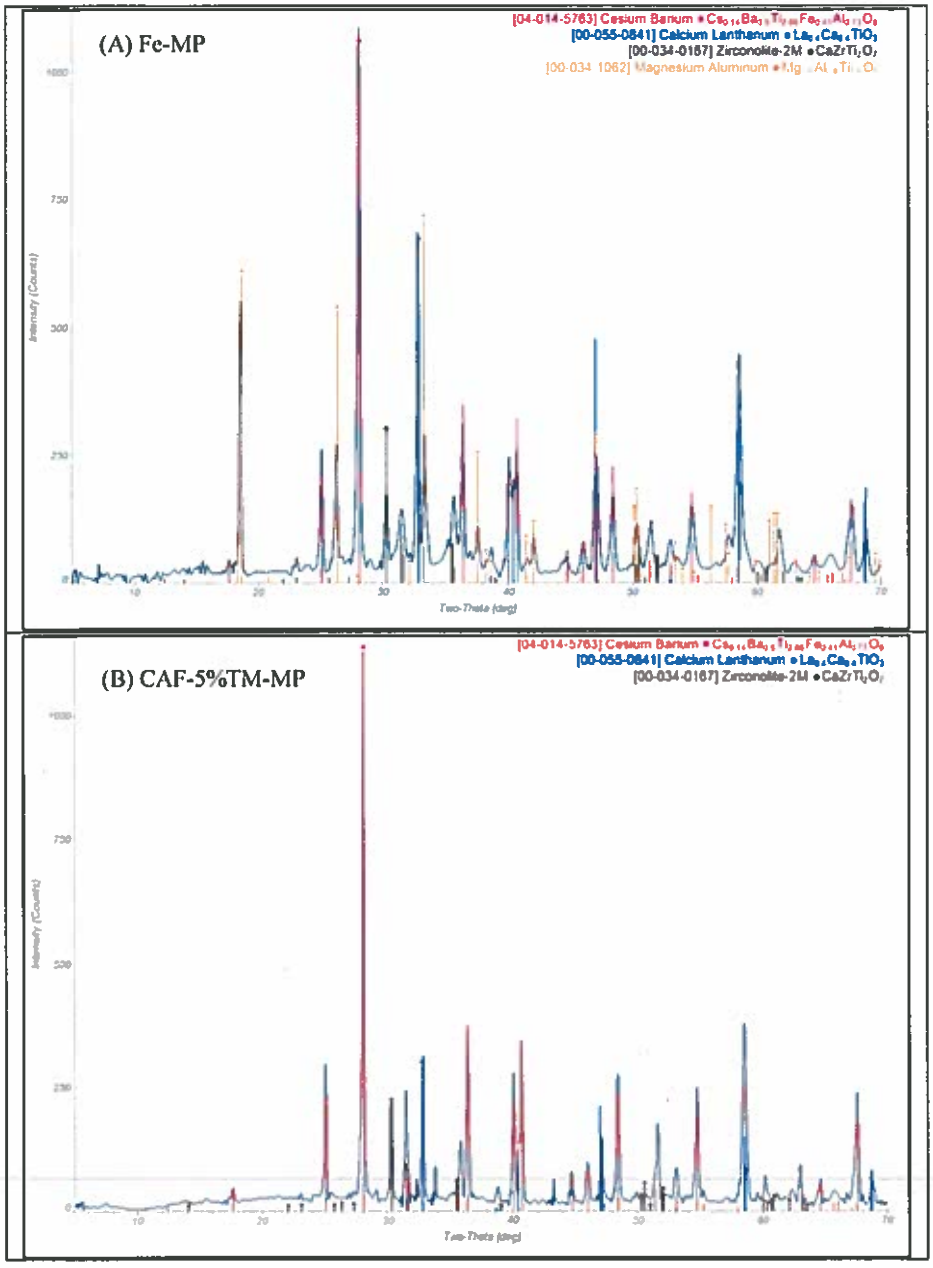

Figure 2. XRD pattern of (A) Fe-MP pour patty and (B) CAF-5%TM-MP pour patty.

3.2. Viscosity

Melt processing information described previously indicated that a crystal phase appeared to be in equilibrium with the melts at high temperatures. Impact of crystallization on the measured viscosity, which is not equal to the true viscosity of the melt, depends on the crystallization process [17]. The effect on the measured viscosity is difficult to predict but, depends on the crystallization process and the stoichiometry of the crystals. However, once crystals impinge, the apparent viscosity will increase due to blocking or interlocking effects and eventually, flow will cease as the sample becomes fully crystalline.

The viscosity was measured to assess the crystallization and melt behavior of the compositions at high temperatures. Figure 3 shows viscosity plotted as ln (η) (in Poise) versus 1/ temperature (in K) for each composition. The plots exhibit a rapid increase in viscosity as a function of temperature at approximately 1375°C for the Fe-MP composition and at approximately 1405°C for the CAF-5%TM-MP composition. These temperatures correspond to viscosities approaching the viscous flow limit and indicate the compositions are fully crystalline (melting temperature) below those temperatures. Although the nature of the melt-crystal composition is unknown, the viscosity behavior appeared reversible in the time span of the measurement as evidenced by the data taken upon re-heating for each composition.

Because the viscosity of melts containing crystallization is complex, the viscosity results alone are helpful for establishing processing parameters but, are incomplete and provide minimal insight into the phenomena governing the viscosity behavior. For example, additional measurements to better understand the nature of the crystalline phase and its solubility in the melt as a function of time *and* temperature would help to establish baseline pouring conditions.

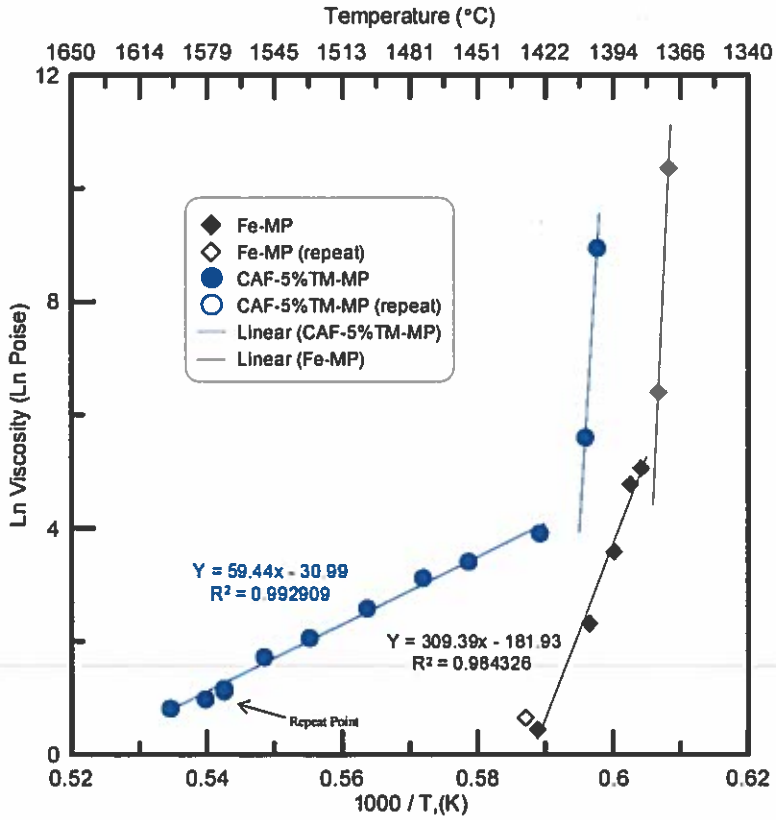

Figure 3. Viscosity relationship of (◆/◇) Fe-MP and (●/○) CAF-5%TM-MP compositions.

3.3. Electrical Conductivity

The results of the electrical conductivity measurements are summarized in Figure 4. The measurement of the electrical conductivity at 1298°C appeared to be an outlier considering the electrical conductivity at temperatures above and below 1298°C. It is possible that conductivity value resulted from measurement uncertainty or may be related to a physical change in the samples, such as crystallization. If it is a result of crystallization, the data suggests that the electrical conductivity lags the crystallization kinetics considering the lower temperature measurement at 905°C was taken several hours after the sample was

isothermally held (compared to 20-30 minute isothermal dwell at the other temperatures). Alternatively, the measurement at 905°C may be an outlier and could indicate a conduction path not intrinsic to the material formed at lower temperatures. An Arrhenius equation of the form

$$\ln(\sigma) = B \times 1/T + A \qquad \textbf{(Equation 1)}$$

where σ is the electrical conductivity in S/m, B is the slope, T is temperature in K, and A is the intercept, was fit to the data excluding the outlier. The Arrhenius relationship was used to calculate the electrical conductivity for selected temperatures listed in Table 2. High temperature (>1450°C) electrical conductivity data collected for SYNROC-type materials measured by comparing the energy characteristics of SYNROC-type material in a CCIM is comparable to the Fe-MP composition [18]. The measured electrical conductivity of the Fe-MP composition was approximately 15-20% greater than the SYNROC-type material. The electrical conductivity determined for Fe-MP is adequate for processing in the CCIM at temperatures above 900°C based on discussions with INL personnel and previous electrical conductivity measurements of SYNROC [18].

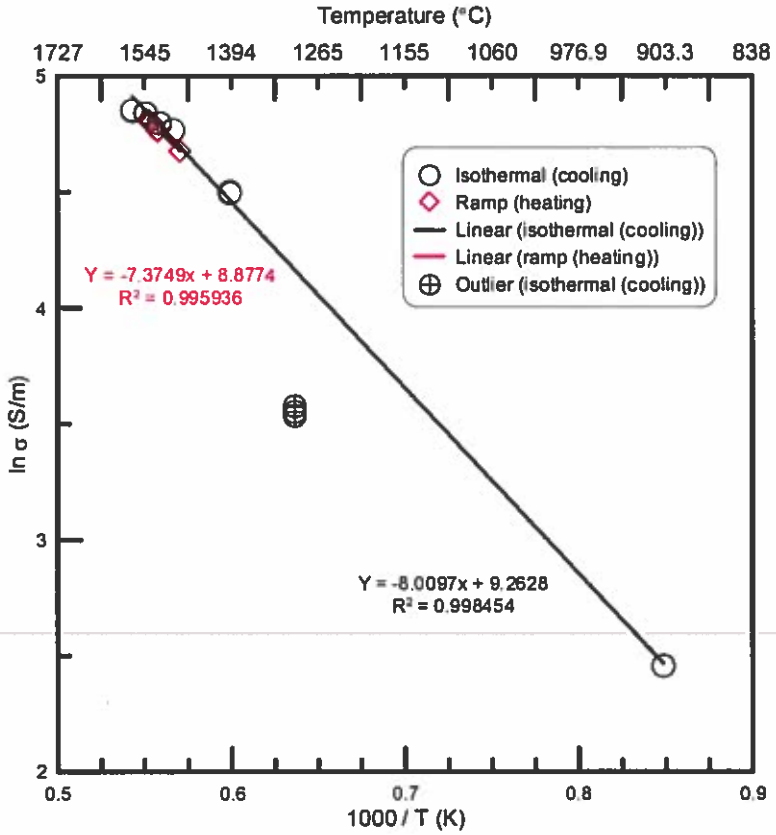

Figure 4. Electrical conductivity of Fe-MP ceramic composition.

Table 2. Calculated electrical conductivity (σ in S/m) as a function of temperature from fitted Arrhenius coefficients for the Fe-MP composition.

Temperature (°C)	900	1000	1100	1200	1300	1400	1500	1600
Conductivity (S/m)	10.3	17.9	28.6	42.9	61.1	83.4	110.0	140.8

3.4. Thermal Analysis

The DTA data is plotted in Figure 5. The Fe-MP composition exhibited two convoluted endotherms and the CAF-5%TM-MP composition exhibited a single endotherm upon heating at approximately 1365°C. The endotherms presumably represent a melting event substantiated by the viscosity data (1375°C – see section 3.2) which coincides well with the DTA data (1365°C), at least for the Fe-MP composition. It is suspected that the melting temperature (1405°C) extrapolated from the viscosity data for the CAF-5%TM-MP composition does not coincide as well with the DTA data because of kinetic effects that will be discussed subsequently.

Similarly, the Fe-MP composition exhibited two convoluted exotherms and the CAF-5%TM-MP composition exhibited a single exotherm upon cooling at approximately 1300°C. The temperature offset between the exotherms and endotherms would not be expected if the two phenomena were related. The source of the temperature offset may be due to the heating rates used for these measurements but, ultimately is unknown.

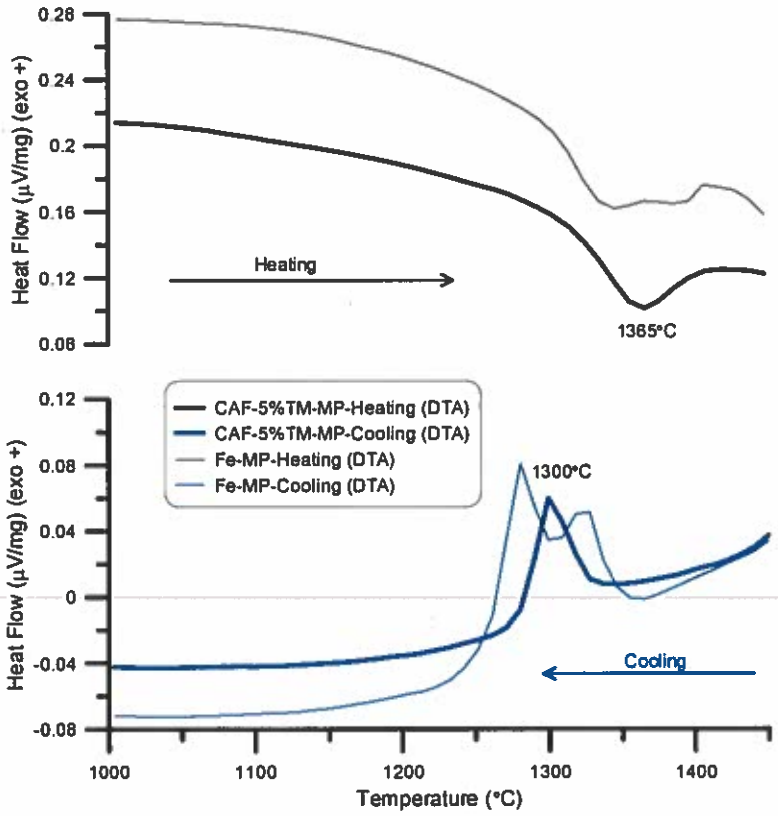

Figure 5. DTA plots for ceramic composition during heating and cooling.

4. CONCLUSIONS & RECOMMENDATIONS

Property data and melting behavior for two crystalline simulated waste forms was presented to support a proof of principle demonstration using INL's CCIM. Given uncertainties in the CCIM capabilities, one waste form designated 'Fe-MP' was designed towards optimized processing and the other, designated 'CAF-5%TM-MP' was designed towards optimized microstructure.

Althoguh stoichiometry and phase transition temperature were comparable for both compositions, the viscosity as a function of temperature and melting behavior were not similar. This suggests similar phase evolution but, fundamental differences in their melting and crystallization kinetics. Such differences are evident in the viscosity data in which the Fe-MP and CAF-5%TM-MP compositions both exhibit Arrhenius behavior below their melting temperatures but, with significantly different rates (slopes). The Fe-MP composition approaches the expected behavior of an ideal crystal (i.e. narrow working temperature range) whereas the CAF-5%TM-MP composition displays evidence of a slower crystallization process (i.e. large working temperature range).

Electrical conductivity results indicated the Fe-MP composition has acceptable conductivity with respect to processing in the CCIM. Electrical conductivity was not measured on the CAF-5%TM-MP composition but, the similarity in compositions would suggest similar electrical conductivities.

The success of processing either ceramic composition will likely depend on the working temperature of the pour spout in the CCIM since the melter can achieve temperatures approaching 1700°C. A pour spout temperature maintained at $\geq$ 1450°C should be sufficient to process the Fe-MP composition. The solid-liquid equilibrium behavior in the CAF-5%TM-MP composition is expected to limit the ability to process it through the CCIM if the *maximum* pour spout temperature is approximately 1450°C.

Based on the limited laboratory scale test results, the Fe-MP composition is recommended to demonstrate proof of principle for processing crystalline simulated waste forms considering the current configuration of INL's CCIM. Understanding the phase assemblage is not ideal in the Fe-MP compositions, if proposed modifications to the CCIM can maintain a nominal temperature of 1600°C throughout the melter, drain, and pour spout, then the CAF-5%TM-MP composition should be considered for a proof of principle demonstration. Raw material batch components for 50 kg of material are provided in Appendix A.

6. REFERENCES

1. Biagioni, C., P. Orlandi, and M. Pasero, *Ankangite from the Monte Arsiccio mine (Apuan Alps, Tuscany, Italy): occurrence, crystal structure, and classification problems in cryptomelane group minerals.* Periodico Di Mineralogia, 2009. **78**(2): p. 3-11.
2. Gunn, D.S.D., et al., *Novel Potentials for Modelling Defect Formation and Oxygen Vacancy Migration in $Gd_2Ti_2O_7$ and $Gd_2Zr_2O_7$ Pyrochlores.* Journal of Materials Chemistry, 2012. **22**(11): p. 4675-4680.
3. Ubic, R., I.M. Reaney, and W.E. Lee, *Perovskite $NdTiO_3$ in Sr- and Ca-doped BaO-Nd_2O_3-TiO_2 Microwave Dielectric Ceramics.* Journal of Materials Research, 1999. **14**(04): p. 1576-1580.
4. Xu, H.F. and Y.F. Wang, *Crystallization Sequence and Microstructure Evolution of Synroc Samples Crystallized from $CaZrTi_2O_7$ Melts.* Journal of Nuclear Materials, 2000. **279**(1): p. 100-106.
5. Aubin-Chevaldonnet, V., et al., *Preparation and Characterization of $(Ba,Cs)(M,Ti)_8O_{16}$ (M = Al^{3+}, Fe^{3+}, Ga^{3+}, Cr^{3+}, Sc^{3+}, Mg^{2+}) Hollandite Ceramics Developed for Radioactive Cesium Immmobilization.* Journal of Nuclear Materials, 2007. **366**(1-2): p. 137-160.
6. Carter, M.L., E.R. Vance, and H. Li, *Hollandite-rich Ceramic Melts for Immobilization of Cs.* Mat. Res. Soc. Symp. Proc., 2004.
7. Carter, M.L., et al., *Mn Oxidation States in $Ba_xCs_yMn_zTi_{8-z}O_{16}$.* Mat. Res. Soc. Symp. Proc., 2004.
8. Brinkman, K., et al., *Crystalline Ceramic Waste Forms: Comparison of Reference Process for Ceramics Waste Form Fabrication.* 2013, Savannah River National Laboratory: Aiken, SC.
9. SRNL, *SRNL Determination of Glass Viscosity.* 2007, Savannah River National Laboratory: Aiken, SC.
10. Schumacher, R.F., R.J. Workman, and T.B. Edwards, *Calibration of the Viscosity of DWPF Start-Up Glass.* 2001, Westinghouse Savannah River Company: Aiken, SC.
11. Schumacher, R.F. and D.K. Peeler, *Establishment of Harrop High-Temperature Viscometer.* 1998, Westinghouse Savannah River Company: Aiken, SC.
12. PNNL, *Electrical Conductivity Measurement.* 2012, Pacific Northwest National Laboratory: Richland, WA.
13. Crum, J.V., et al., *DWPF Startup Frit Viscosity Measurement Round Robin Results.* J. Am. Ceram. Soc., 2012. **95**(7): p. 2196–2205.
14. SRNL, *Use of the Netzsch STA 409 PC Luxx DTA/TGA System.* 2012, Savannah River National Laboratory: Aiken, SC.
15. Brinkman, K., et al., *Development of Crystalline Ceramics for Immobilization of Advanced Fuel Cycle Reprocessing Wastes.* 2012, Savannah River National Laboratory: Aiken, SC.
16. Brinkman, K., K. Fox, and M. Tang, *Development of Crystalline Ceramics for Immobilization of Advanced Fuel Cycle Reprocessing Wastes.* 2011, Savannah River National Laboratory: Aiken, SC.
17. Shelby, J.E., *Introduction to Glass Science and Technology.* 1997, Cambridge, UK: The Royal Society of Chemistry.
18. Knyazev, O.A. and S.V. Stefanovskii, *Determination of Melt Electrical Resistivity of IMCC*, in *Waste Management Conference.* 2001: Tucson, AZ.

Appendix A
Raw Material Batch Sheets

Raw Material Batch Sheets for 50 kg of reacted feed

Component	Source	Amount Needed (g)	
		Fe-MP	CAF-5%TM-MP
Al_2O_3	Al_2O_3	0.000	627.122
$CaO^{\dagger}$	$CaCO_3$	1224.233	1561.037
CdO	CdO	54.405	56.357
Cr_2O_3	Cr_2O_3	0.000	3116.102
Eu_2O_3	Eu_2O_3	85.096	83.951
Fe_2O_3	Fe_2O_3	7564.137	3273.922
Gd_2O	Gd_2O	79.516	78.446
$SrO^{\dagger}$	$SrCO_3$	693.638	684.311
TiO_2	TiO_2	24326.010	24741.113
ZrO_2	ZrO_2	1478.710	1531.767
$BaO^{\dagger}$	$BaCO_3$	8128.208	8091.548
Ce_2O_3	Ce_2O_3	1610.772	1589.112
$Cs_2O^{\dagger}$	Cs_2CO_3	1648.347	1626.182
La_2O_3	La_2O_3	783.995	773.453
MoO_3	MoO_3	418.503	412.875
Nd_2O_3	Nd_2O_3	2589.138	2554.321
$Pr_2O_3^{\ddagger}$	Pr_6O_{11}	740.224	730.270
SeO_2	SeO_2	40.455	41.907
SnO_2	SnO_2	34.875	36.127
Sm_2O_3	Sm_2O_3	532.894	525.728
TeO_2	TeO_2	325.037	336.700
Y_2O_3	Y_2O_3	311.087	322.249
$Rb_2O^{\dagger}$	Rb_2CO_3	258.515	267.790

† Source component was in the form of carbonate.
‡ Source component was in the form of a different oxide.